Journal of Autoimmunity 97 (2019) 40–47

Contents lists available at ScienceDirect

Journal of Autoimmunity

journal homepage: www.elsevier.com/locate/jautimm

Autoimmunity risk- and protection-associated *IL7RA* genetic variants differentially affect soluble and membrane IL-7Rα expression

Christian Lundtoft[a], Julia Seyfarth[a,b], Sonja Oberstrass[a], Joachim Rosenbauer[b,c], Christina Baechle[b,c], Michael Roden[d,e], Reinhard W. Holl[b,f], Ertan Mayatepek[a], Sebastian Kummer[a], Thomas Meissner[a,b], Marc Jacobsen[a,*]

[a] Department of General Pediatrics, Neonatology and Pediatric Cardiology, University Children's Hospital, Medical Faculty, 40225, Duesseldorf, Germany
[b] German Center for Diabetes Research (DZD), 85764, Munich-Neuherberg, Germany
[c] Institute for Biometrics and Epidemiology, German Diabetes Center, Leibniz Center at Heinrich-Heine University Düsseldorf, 40225, Düsseldorf, Germany
[d] Division of Endocrinology and Diabetology, Medical Faculty, Heinrich Heine University Düsseldorf, 40225, Düsseldorf, Germany
[e] Institute for Clinical Diabetology, German Diabetes Center, Leibniz Center at Heinrich-Heine University Düsseldorf, 40225, Düsseldorf, Germany
[f] Institute of Epidemiology and Medical Biometry, ZIBMT, University of Ulm, 89081, Ulm, Germany

ARTICLE INFO

Keywords:
T cells
IL-7
IL-7 receptor α-chain
rs1494558
rs6897932

ABSTRACT

Interleukin-7 receptor α-chain (*IL7RA*) haplotypes are associated with susceptibility to autoimmune diseases including type 1 diabetes (T1D). Previous studies found lower soluble IL-7Rα (sIL-7Rα) serum levels of the protection-associated *IL7RA* haplotype assumed to reduce IL-7 availability for self-reactive T cells. Also, a risk-associated *IL7RA* haplotype is accompanied by lower sIL-7Rα serum concentrations but no underlying mechanisms have been described and the causative polymorphism remains unknown.

Here, we characterized functional implications of the nonsynonymous rs1494558 (Thr66Ile), which tags the protection-associated *IL7RA* haplotype, in HEK293T cells and serum samples of T1D patients with different haplotype carriers. Influence of risk- and protection-associated haplotypes on IL-7Rα was analyzed.

The risk-associated Ile66 variant affected gel mobility and impaired secretion of the sIL-7Rα as well as expression of the membrane-associated (m)IL-7Rα in HEK293T cells. Serum sIL-7Rα analyses confirmed differential gel mobility of the Ile66 variant and found decreased sIL-7Rα serum levels of T1D patients carrying the Ile66-tagged haplotype. Differences in glycosylation were not causative for differential mobility but enhanced the effects on impaired secretion. Comparison of protection- and risk-associated haplotypes in a cell line-based *in vitro* model identified dominant effects of the protective haplotype tagged by rs6897932 (Ile244) on mIL-7Rα expression, whereas the risk haplotype mainly affected the sIL-7Rα.

This study identified novel functional effects of the Ile66 *IL7RA* variant and characterized features of autoimmunity risk- and protection-associated haplotypes. The findings add to our understanding of how these haplotypes regulate sIL-7Rα and mIL-7Rα expression in T cells causing differential susceptibility to autoimmune diseases.

1. Introduction

Interleukin (IL)-7 is an important factor for T-cell function including homeostatic proliferation and survival [1]. In addition, IL-7 promotes the generation of self-reactive T cells and contributes to development of autoimmune diseases like multiple sclerosis or type 1 diabetes (T1D) [2]. IL-7 is primarily produced by stromal cells and has been shown to be largely stable in the circulation [3]. IL-7-availability is regulated by consumption of IL-7-dependent cells (mainly T cells and innate lymphoid cells ILCs) [3]. The IL-7 receptor (composed of the IL-7Rα and the common-γ chain receptor) plays a central role in the regulation of IL-7 availability and its expression is tightly regulated [4]. Soluble (s) IL-7Rα and membrane-associated (m)IL-7Rα are generated by alternative splicing, and both contribute to IL-7-availability. A functional role of both sIL-7Rα and mIL-7Rα in development of autoimmune diseases has been suggested [5–8].

IL7RA single nucleotide polymorphisms (SNPs) were found to be associated with susceptibility for autoimmune diseases [9,10]. Specific

* Corresponding author. Department of General Pediatrics, Neonatology, and Pediatric Cardiology, University Children's Hospital, Moorenstr. 5, 40225, Duesseldorf, Germany.
E-mail address: marc.jacobsen@med.uni-duesseldorf.de (M. Jacobsen).

https://doi.org/10.1016/j.jaut.2018.10.003
Received 10 October 2018; Accepted 11 October 2018
Available online 17 October 2018
0896-8411/

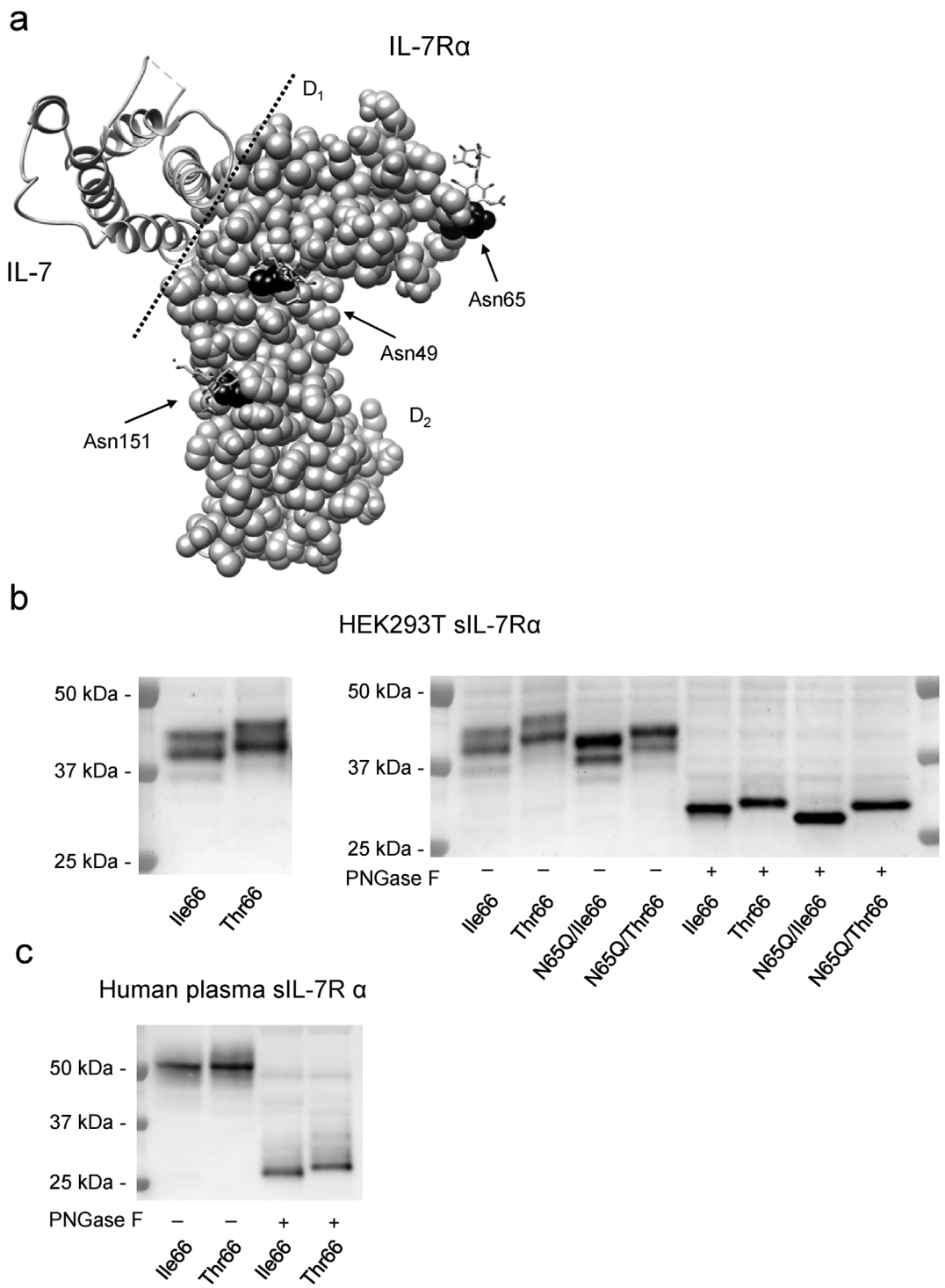

Fig. 1. The nonsynonymous SNP rs1494558 (Thr66Ile) affects gel mobility of sIL-7Rα. (a) Crystal structure of the ectodomain of IL-7Rα (sphere view) and IL-7 (ribbon diagram). Three N-glycosylation sites identified in the crystal structure are shown in black for the D_1 and D_2 domains. Structure generated in Chimera version 1.10.2 from PDB id 3DI3 [17]. (b) Western blots of cell lysate from HEK293T cells transfected with sIL-7Rα coding Ile66 or Thr66. Two sIL-7Rα variants mutated in position 65 (N65Q) to prevent N-glycosylation were included, and all samples were analyzed with or without PNGase F-treatment to remove N-glycans. (c) sIL-7Rα enriched from human plasma from healthy donors homozygous for Ile66 or Thr66 was analyzed by western blot with or without PNGase F-treatment.

IL7RA haplotypes tagged by known SNPs confer increased risk (termed 'risk allele' throughout this manuscript) or protection (termed 'protective allele') [9,11,12]. Functional mechanisms are so far only described for the protective allele tagged by rs6897932T (coding for Ile244) variant in *IL7RA* exon 6 [9]. The protective allele impairs *IL7RA* alternative splicing and causes decreased sIL-7Rα secretion [9], leading to generally lower sIL-7Rα serum levels [7]. In autoimmune pathology, e.g. in patients with multiple sclerosis or T1D, lower sIL-7Rα serum concentrations are accompanied by lower total IL-7 levels [7,13], whereas this was not found for healthy individuals [7]. Therefore, differential sIL-7Rα serum concentrations are not solely accountable for IL-7 consumption and additional mechanisms likely contribute. Own previous studies strengthened this assumption, showing that lower sIL-7Rα serum levels are also present in T1D patients carrying the risk

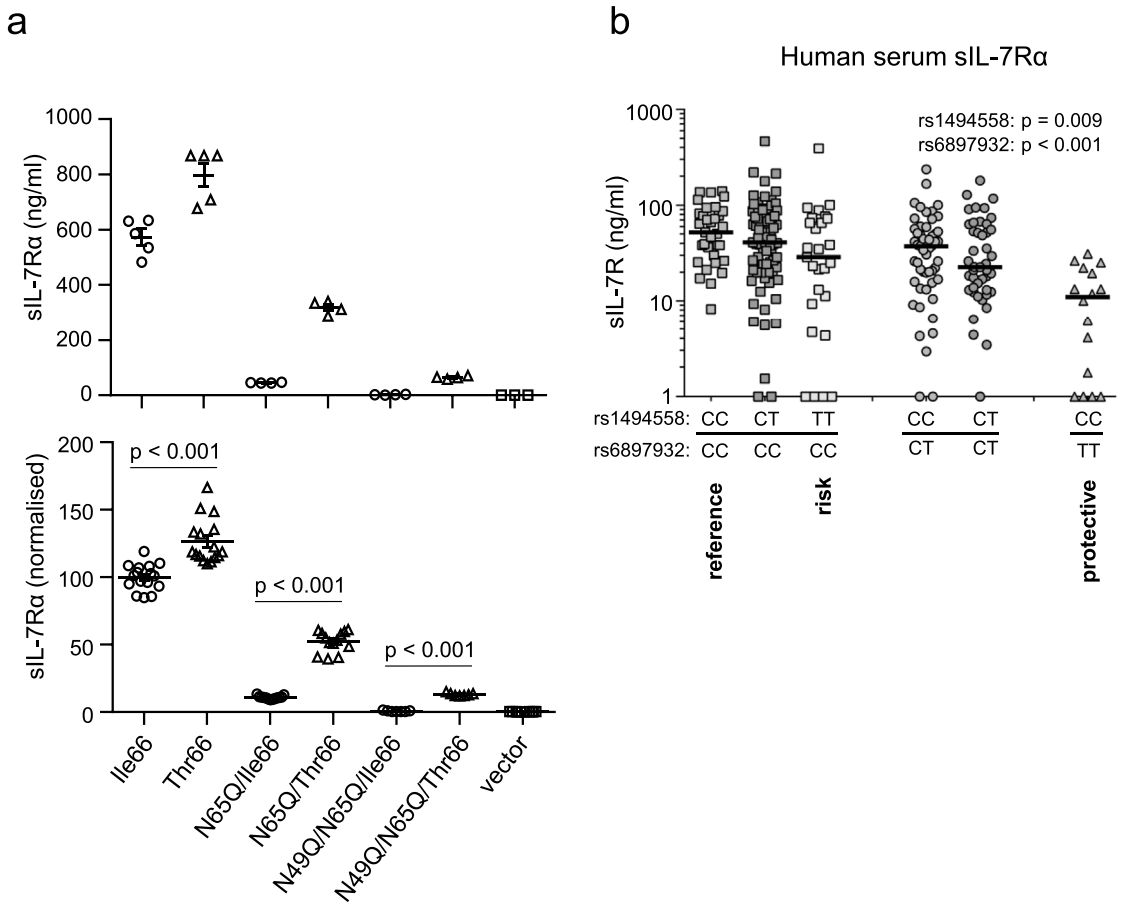

Fig. 2. Ile66 influences sIL-7Ra secretion and α serum levels of sIL-7Rα from T1D patients. (a) sIL-7Rα concentrations of culture supernatants from HEK293T cells transfected with different sIL-7Rα variants measured by cytometric bead array are shown. In addition to a variant mutated in position 65 (N65Q), a second variant also deficient for N-glycosylation in position 49 (N49Q) and HEK cells transfected with empty vector have been included. sIL-7Rα concentrations from one representative experiment (upper panel), and concentrations of sIL-7Rα variants normalized to transfection efficacy (i.e. geometric mean of eBFP expression) (lower panel) are shown. Combined and normalized results from four (Ile66, Thr66, N65Q/Ile66 and N65Q/Thr66) or two (N49Q/N65Q/Ile66 and N49Q/N65Q/Thr66) experiments are shown, and the average sIL-7Rα in Ile66 samples was set to 100. Data were analyzed by ANOVA. (b) sIL-7Rα was analyzed in serum from patients with T1D and plotted according to the genotypes of rs1494558 and rs6897932. The overall effect of the individual SNPs on sIL-7Rα serum concentration was analyzed by linear regression of log-transformed data. Association of haplotypes to autoimmune disease (i.e. risk, protective and reference haplotype) is indicated. Mean values ± SEM are shown.

allele tagged by rs1494555 [13]. In contrast to the Ile244 variant, decreased sIL-7Rα serum levels in T1D patients carrying the rs1494555 risk allele were not associated with lower IL-7 serum levels and a correlation between sIL-7Rα/IL-7 serum concentration was not found [13]. The rs1494555 SNP is in strong linkage disequilibrium with the SNP rs1494558 ($r^2 = 0.97$). The rs1494558 risk allele codes for the non-synonymous Ile66 in the extracellular domain of the IL-7Rα.

The underlying hypothesis for this study was that rs1494558 variants affects IL-7Rα expression and/or function, and that concomitant analysis of rs1494558 and rs6897932 variants may gain insight into differential effects on sIL-7Rα and mIL-7Rα expression. We used HEK293T cell lines for transfection experiments and confirmed results of sIL7R expression by analyses of serum samples from T1D patients.

2. Methods

2.1. Study participants

SNP and serum analyses were performed in a cohort of children and adolescents with T1D recruited for the Pediatric Diabetes Biobank within the German Center for Diabetes Research (DZD Biobank) as previously described [13]. The ethics committee of the medical faculty, Heinrich- Heine-University Duesseldorf approved this study (ID 4844). Written informed consent was received from all donors (older than 14 years) and the legal guardians.

2.2. Genotyping of IL7RA single nucleotide polymorphisms

DNA was isolated from whole blood using QIAamp DNA Mini kit (Qiagen) followed by genotyping with predesigned TaqMan SNP Genotyping Assays (Applied Biosystems) and analyzed on a 7500 Real-Time PCR machine (Applied Biosystems). A call rate > 98% was found for the SNPs, and none of the SNPs deviated from the Hardy–Weinberg equilibrium.

2.3. Cytometric bead assay for sIL-7Rα quantification

Measurement of sIL-7Rα from serum has been described in detail previously [14], and was performed with minor modifications for culture supernatants. Briefly, functional beads (Bead A4, BD Biosciences) were conjugated with polyclonal anti-human IL-7Rα (R&D Systems) according to manufacturer's protocol. Samples and standard (rhIL-7Rα-Fc Chimera Protein, R&D Systems) were diluted in culture medium and incubated with anti-IL-7Rα-conjugated beads. Bound sIL-7Rα was detected using biotinylated mouse anti-human IL-7Rα (clone HIL-7R-M21, BD Biosciences) and Streptavidin PE (BioLegend). Beads were

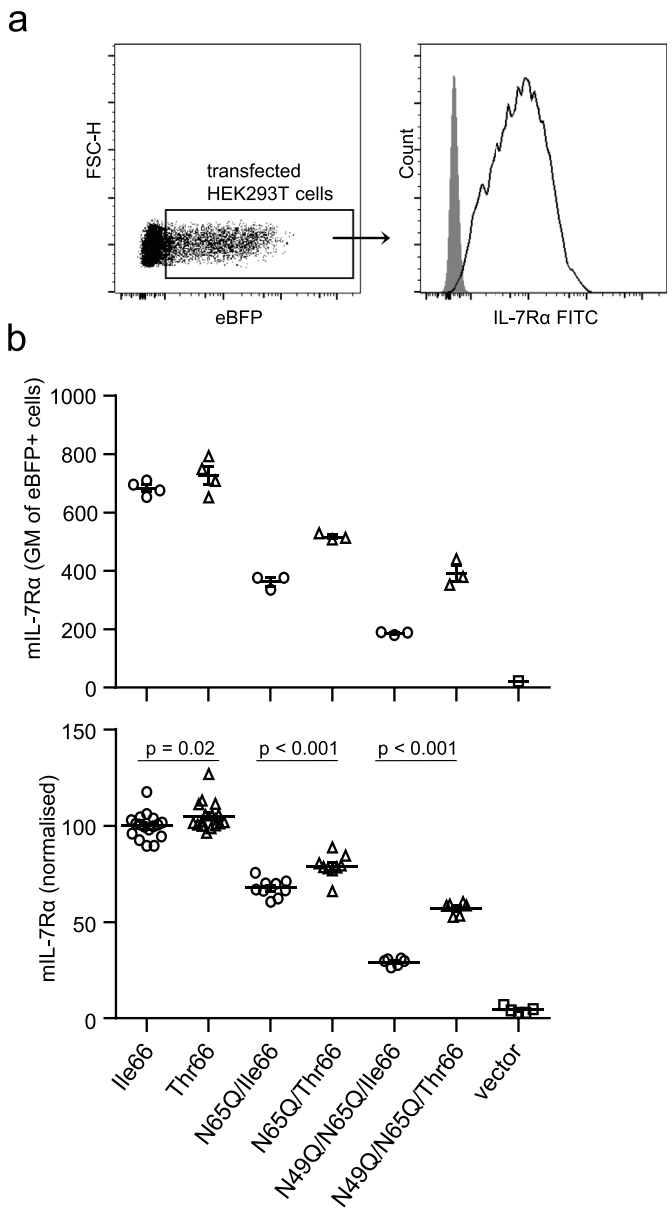

Fig. 3. Membrane-associated (m)IL-7Rα level on HEK293T cells transfected with *IL7RA* Ile66 or Thr66 and N-glycosylation-deficient mutants (a) Gating procedure of mIL-7Rα transfected (i.e. eBFP-positive). HEK293T cells (left panel) and mIL-7Rα-specific antibody staining (right panel; Ile66: open black line; vector control; shaded grey). (b) Surface expression of mIL-7Rα on eBFP-positive HEK293T cells after transfection (for 24 h) with different *IL7RA* variants measured by fluorescence levels (geometric mean (GM) of IL-7Rα expression). Variants deficient in N-glycosylation at position 65 (N65Q) and position 49 (N49Q) are included together with HEK293T cells transfected with empty vector. mIL-7Rα expression levels from one representative experiment are shown (upper panel) together with normalized levels of mIL-7Rα according to transfection efficacy (i.e. GM of IL-7Rα/GM of eBFP) combined from repeated experiments. The average mIL-7Rα in Ile66 samples was set to 100. Combined results from five (Ile66 and Thr66), three (N65Q/Ile66, N65Q/Thr66) or two (N49Q/N65Q/Ile66 and N49Q/N65Q/Thr66) representative experiments are shown. Data analyzed by ANOVA.

analyzed on a BD LSRFortessa flow cytometer (BD Biosciences), and sIL-7Rα concentration was computed from median PE values by 4-parametric regression in GraphPad Prism version 6.07.

Table 1
IL7RA haplotypes and described association with multiple sclerosis (MS).

haplotype	rs1494558		rs6897932		Frequency (%)[b]	MS association[a]
Ile66/Thr244	T	Ile66	C	Thr244	29.7	risk
Thr66/Thr244	C	Thr66	C	Thr244	42.6	reference
Ile66/Ile244	T	Ile66	T	Ile244	NA	NA
Thr66/Ile244	C	Thr66	T	Ile244	27.1	protection

[a] Multiple sclerosis (MS) risk association based on Gregory *et* al. (2007).
[b] Frequency according to 1000 genomes project, (i.e. EUR population [CEU, TSI, FIN, GBR and IBS combined], n = 503); NA: not applicable.

2.4. Cloning of vectors

mIL-7Rα and sIL-7Rα corresponding to the NCBI Reference Sequences (NM_002185.4 and XM_005248299.3, respectively) were cloned from human mRNA and inserted into LeGO-iB2 vector (generated from LeGO-iG2 by exchanging eGFP for eBFP) [15] using the *Eco*RI/*Not*I (mIL-7Rα) or *Bam*HI-*Bgl*II/*Not*I (sIL-7Rα) restriction enzyme sites (all restriction enzymes from Thermo Fisher Scientific). A mIL-7Rα construct containing the complete introns upstream and downstream of exon 6 (see Fig. 4a) was generated from human mRNA and DNA by multiple PCR reactions and inserted into LeGO-iG2 using the *Bam*HI-*Bgl*II/*Not*I restriction enzyme sites. The sequence corresponds to the NCBI Reference Sequences (NM_002185.4 for exons and NG_009567.1 for introns). A Kozak sequence (GCCACC) was introduced upstream of the start codon of all constructs. To generate mutants of mIL-7Rα and sIL-7Rα, PCR was performed with Phusion High-Fidelity PCR Master Mix with GC Buffer (New England BioLabs) and appropriate primers. The reactions were run for 30 s at 98 °C followed by 18 cycles of 7s at 98 °C, 30 s at 60 °C and 8 min at 72 °C, followed by 10 min at 72 °C. Plasmid of bacterial origin was removed by *Dpn*I digestion prior to transformation. Successful mutation was verified by DNA sequencing. Primers for cloning and mutations are listed in Supplementary Table 1.

2.5. Cell culture and transfection

HEK293T cells were grown in Dulbecco's Modified Eagle's Medium (high glucose, GlutaMAX, pyruvate) supplemented with 10% heat-inactivated FCS, 25 mM HEPES (all Thermo Fisher Scientific), 100 units penicillin/ml and 100 µg streptomycin/ml (Sigma Aldrich). Transfections were performed in medium supplemented with 25 µM Chloroquine (Sigma Aldrich) using the Calcium Phosphate Transfection Kit (Sigma Aldrich).

2.6. Flow cytometry analysis of receptor expression

Cells were harvested and stained with Viability Dye eFluor 780 (eBioscience) and mouse anti-human IL-7Rα AF647 (clone HIL-7R-M21, BD Biosciences), or polyclonal goat anti-human IL-7Rα (R&D Systems) followed by FITC-conjugated polyclonal donkey anti-goat IgG (R&D Systems). After staining, cells were fixed with Fixation Buffer (BioLegend) and analyzed using an LSRFortessa flow cytometer (BD Biosciences). The two IL-7Rα antibodies (polyclonal and clone HIL-7R-M21) showed similar performance independent from the mutations of IL-7Rα (Supplementary Fig. 1).

2.7. Protein preparation for western blot

Proteins from cell lysate was isolated using CelLytic M supplemented with Protease Inhibitor Cocktail (Sigma Aldrich), and protein concentration was determined with Protein Assay Dye Reagent (Bio-Rad) using BSA as standard (Sigma Aldrich). 20 µg protein was heated 10 min at 100 °C in Glycoprotein Denaturing buffer (New England BioLabs). In some experiments, protein was added PNGase F to remove

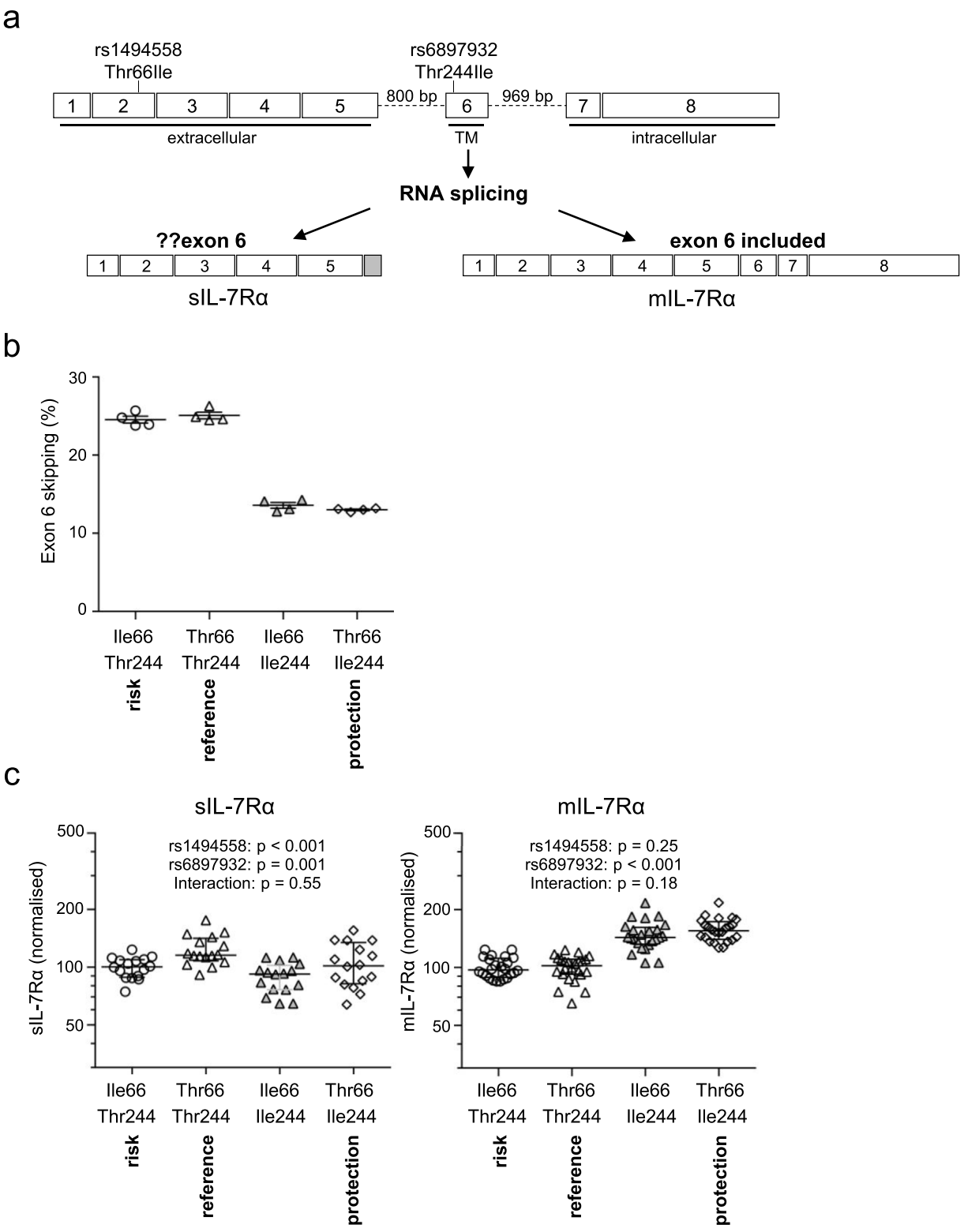

Fig. 4. Ile244 in exon 6 of *IL7RA* dominantly modulates mIL-7Rα expression. (a) A construct containing all 8 exons of IL-7Rα including introns upstream and downstream of exon 6 was generated, thereby allowing for alternative splicing of the construct. In addition, the nonsynonymous SNPs rs1494558 (Thr66Ile) and rs6897932 (Thr244Ile) were introduced. (b) Proportion of exon 6-skipping relative to total IL-7Rα mRNA of the constructs generated in (a), when overexpressed in HEK293T cells. The level of Δ6 IL-7Rα and full-length IL-7Rα was analyzed by PCR followed by separation of the PCR products on an agarose gel. (c) sIL-7Rα in culture medium (left panel) and mIL-7Rα on HEK293T cells (right panel) 24 h after transfection with the IL-7Rα constructs from (a). sIL-7Rα and mIL-7Rα levels were normalized as described in Figs. 2 and 3, respectively. Combined results from four (sIL-7Rα) and six (mIL-7Rα) independent experiments are shown, each point representing one individual transfection. Data analyzed by ANOVA. Association of haplotypes to autoimmune disease (risk, protective, and reference haplotype) is indicated.

N-glycans, while a combination of O-Glycosidase, α2-3,6,8,9 Neuraminidase A, β-N-acetylhexosaminidase f and β1-4 Galactosidase S was used in combination to trim and remove O-glycans according to manufacturer's protocol (New England BioLabs). After enzymatic treatment, samples were heated for 10 min at 80 °C and loaded on a NuPAGE 4–12% Bis-Tris gels (all Thermo Fisher Scientific) together with Precision Plus Protein Standards All Blue (Bio-Rad). Run in NuPAGE MOPS Buffer (Thermo Fisher Scientific) at 100 V. After separation, proteins were blotted to a 0.2 μm nitrocellulose membrane (Bio-Rad) in NuPAGE Transfer Buffer (Thermo Fisher Scientific) at 4 °C for 2 h at 240 mA. Membrane was blocked in 5% skim milk (Sigma Aldrich) in PBS/T (PBS, 0.1% Tween-20), incubated overnight at 4 °C with polyclonal goat anti-human IL-7Rα (R&D Systems, 1:2000 in PBS/T/2% skim milk). HRP Rabbit anti-Goat IgG (H + L) (invitrogen, 1:2000 in PBS/T/2% skim milk) was used as secondary antibody, and the membrane was developed using BM Chemiluminescence Western Blotting Substrate (POD) (Sigma Aldrich) on a ChemiDoc Touch Imaging System (Bio-Rad).

2.8. Capture of sIL-7Rα from human plasma

10 ml plasma from donors homozygous for rs1494558 (CC or TT) was incubated overnight with biotinylated anti-human IL-7Rα (clone HIL-7R-M21) at 4 °C. Streptavidin Magnetic Beads (New England Biolabs) was added followed by overnight incubation at 4 °C. Subsequently, beads were captured magnetically, and bound protein was detached by adding Glycoprotein Denaturing Buffer (New England BioLabs) by incubation 10 min at 100 °C, followed by SDS-PAGE and western blot.

2.9. mRNA analysis of transfected HEK293T cells

mRNA was isolated from HEK293T cells transfected with the splicing IL-7Rα construct using the NucleoSpin RNA kit (Macherey-Nagel) with subsequent synthesis of cDNA using Maxima H Minus First Strand cDNA Synthesis kit (Thermo Fisher Scientific). PCR was performed with Phusion High-Fidelity PCR Master Mix with GC Buffer (New England BioLabs) (see PCR primers in Supplementary Table 1). The reactions were run for 30 s at 98 °C followed by 25 cycles of 7s at 98 °C, 15 s at 60 °C and 45 s at 72 °C, followed by 8 min at 72 °C. PCR products were mixed with GelPilot 5x Loading dye (Qiagen) and separated on a 1% Agarose gel (BioBudget) in TBE buffer added 0.007% GelRed (Biotium) at 100 V. Subsequently, the gel was analyzed on a ChemiDoc Touch Imaging System (Bio-Rad).

2.10. Statistical analysis

Haplotypes of selected SNPs in *IL7RA* were predicted from 1000 Genomes data set using HaploView version 4.2. Statistical analyses were performed in R version 3.3.0, applying ANOVA of square root-transformed data. Overall effect of SNPs on serum sIL-7Rα was evaluated by linear regression of log-transformed data using *haplo.glm* from the package *SNPassoc* [16]. Plots were generated in GraphPad Prism version 6.07. Two-tailed p-values < 0.05 were considered significant.

3. Results

3.1. The IL-7Rα Ile66 variant affected IL-7Rα gel mobility

The nonsynonymous rs1494558 SNP codes for an amino acid exchange (i.e. Thr66Ile) in the ectodomain region distant from the IL-7-binding site of the IL-7Rα chain (Fig. 1a). Initially, we over-expressed Thr66Ile alleles of the sIL-7Rα in HEK293T cells. Western blot analyses indicated effects on gel mobility for sIL-7Rα variants with Ile66 being detected at a lower position (Fig. 1b; left). Located next to the Asn65 N-glycosylation site [17,18], we investigated the influence on N-glycosylation as a potential cause for differential gel mobility. Differences in gel positions, however, were still present after removal of N-glycans from cell lysate (Fig. 1b; right). To exclude that N-glycosylated Asn65 could be resistant to enzymatic deglycosylation, we generated sIL-7Rα N65Q variants incapable of N-glycosylation at position 65. As expected, a reduction in molecular weights was seen for the N-glycosylation-defective N65Q mutants, but the differences between Thr66 and Ile66 were still apparent (Fig. 1b; right). O-glycosidase treatment excluded that O-glycosylation of Thr66 was the reason for different mobility (Supplementary Fig. 2). Next, we enriched sIL-7Rα of plasma from homozygous human Thr66 and Ile66 carriers to confirm that differences are detectable *ex vivo*. Minor differences in gel mobility were found and deglycosylation confirmed the lower position of sIL-7Rα Ile66 from plasma (Fig. 1c). We concluded that the protective Ile66 allele affected gel mobility of the sIL-7Rα indicating glycosylation-independent conformational differences.

3.2. The Ile66 variant impaired sIL-7Rα secretion in vitro and caused lower sIL-7Rα serum concentrations in T1D patients

Conformational changes may affect protein transport and secretion. Hence, we investigated Thr66Ile effects on sIL-7Rα secretion. Since N-glycosylation of the D_1 domain of type I cytokine receptors has proven important for receptor trafficking [19,20], we included mutants defective for N-glycosylation in the D_1 domain of IL-7Rα (i.e. N49Q and N65Q) as controls. Ile66-transfected HEK293T cells showed markedly reduced sIL-7Rα secretion compared to Thr66-transfected cells (Fig. 2a; upper graph). This difference persisted also in the absence of glycosylation, although sIL-7Rα secretion was almost completely abrogated under these conditions (Fig. 2a; upper graph). Comparisons of repetitive experiments including normalized sIL-7Rα concentrations revealed significantly impaired secretion of sIL-7Rα for Ile66 ($p < 0.001$ for all comparisons; Fig. 2a; lower graph).

We demonstrated previously that the rs1494555 allele affected sIL-7Rα serum levels [21]. As rs1494555 and rs1494558 alleles are strongly linked but not completely identical, we next compared sIL-7Rα serum concentrations of T1D patients classified rs1494558 and rs6897932 alleles. IL-7Rα protective allele (i.e. rs6897932T, Ile244) carriers had significantly lower sIL-7Rα serum concentrations ($p < 0.001$ to the reference allele; Fig. 2b), and also risk allele carriers (i.e. rs1494558T, Ile66) had lower sIL-7Rα serum concentrations as compared to the reference ($p = 0.009$; Fig. 2b). Therefore, impaired trafficking/secretion of Ile66 in HEK293T cell lines is reflected by lower sIL-7Rα serum concentrations in T1D patients carrying the *IL7RA* risk allele.

3.3. The Ile66 variant impaired mIL-7Rα expression

To determine potential effects on mIL-7Rα expression, HEK293T cells were transfected with mIL-7Rα containing Thr66 or Ile66. We compared transfected HEK293T cells (eBFP-positive) for mIL-7Rα expression (i.e. geometric mean fluorescence intensity of IL-7Rα-specific antibody binding) (Fig. 3a). Although less pronounced than for sIL-7Rα, lower surface mIL-7Rα expression was seen for Ile66 as compared to Thr66 (Fig. 3b; upper graph). As seen for sIL-7Rα variants lacking N-glycosylation showed even more pronounced differences (Fig. 3b; upper graph). Impaired mIL-7Rα expression of Ile66 containing HEK293T cells was significant when comparing repeated normalized experiments (Fig. 3b; lower graph). We concluded that Ile66 also causes diminished mIL-7Rα expression on the cell surface.

3.4. Autoimmunity risk- and protection-associated IL7RA SNPs Thr66Ile and Thr244Ile differ in their effects on mIL-7Rα and sIL-7Rα expression

As mentioned before, *IL7RA* risk or protective alleles for autoimmunity are tagged by Ile66 or Ile244, respectively. Three of four

theoretically possible allele combinations exist (Table 1), with Ile66/Thr244 being the 'risk' haplotype, Thr66/Ile244 being the 'protective' haplotype, and Thr66/Thr244 without known association (termed 'reference') (Table 1). We included all four haplotypes and designed a construct containing all *IL7RA* exons including the complete introns upstream and downstream of exon 6 (Fig. 4a). This allowed concomitant measurement of the rs6897932 allele mediated effects on alternative splicing and of the rs1494558 allele on sIL-7Rα secretion and mIL-7Rα expression in HEK293T cells. mRNA analyses showed reduced exon 6 splicing only in the presence of Ile244 (Fig. 4b), corresponding to previous literature showing impaired splicing of exon 6 and lower sIL-7Rα secretion for this allele. In accordance, secretion of sIL-7Rα was decreased from HEK293T cells carrying the Ile244 ($p < 0.001$) (Fig. 4c; left graph). Ile66 also had diminishing effects on sIL-7Rα protein levels ($p < 0.001$) although moderately lower as compared to Ile244 ($p = 0.06$) (Fig. 4c; left graph). Notably, comparison of mIL-7Rα expression showed marked effects of Ile244 ($p < 0.001$), whereas Ile66 effects were not significant ($p = 0.25$) (Fig. 4c; right graph). Both the marked effect of Ile244 on mIL-7Rα expression and comparable effects of risk and protective alleles on sIL-7Rα secretion challenge suggested mechanisms underlying IL-7-mediated T-cell effects and association with autoimmunity.

4. Discussion

The IL-7Rα Ile66 risk allele was found to impair trafficking and secretion of the sIL-7Rα *in vitro*, and to cause lower sIL-7Rα serum levels in T1D patients. This way we demonstrated that autoimmunity risk- and protection-associated SNPs caused decreased sIL-7Rα secretion by different mechanisms. Whereas differential alternative splicing of the *IL7RA* exon 6 leads to for decreased sIL-7Rα secretion in carriers of the protective Ile244 allele [7,9], we identified IL-7Rα conformational changes due to the nonsynonymous rs1494558T exchange. Conformational changes indicated by different gel mobility persisted after deglycosylation and was detectable in N-glycosylation-deficient mutants expressed in HEK293T cells. We confirmed these findings by analyzing gel mobility of human serum sIL-7Rα of different rs1494558 allele carriers. In addition, we found decreased secretion of the sIL-7Rα and expression of the mIL-7Rα. Because of the well-known importance of glycosylation for intracellular trafficking of the IL-21 receptor and the common-γ chain receptor [19], we assumed that the IL-7Rα Ile66 variant impaired IL-7Rα intracellular trafficking especially under glycosylation-deficient conditions. The Ile66 amino acid exchange is located in an IL-7Rα region distant from the IL-7 binding site, rendering differences in IL-7 binding affinities unlikely. However, since conformational changes were not further characterized as part of this study, functional experiments are needed to address Ile66 effects on IL-7Rα/IL-7 binding.

The role of the sIL-7Rα for IL-7 availability and T-cell functions has been a matter of intensive investigations during the past years. Several studies in the field of autoimmunity were performed, inspired by the association of *IL7RA* SNPs with autoimmune disease susceptibility [9]. These studies demonstrated that increased IL-7 availability due to higher sIL-7Rα levels (i.e. maintenance of an IL-7 reservoir) promoted auto-reactive T cells [7], whereas lower sIL-7Rα levels (e.g. caused by the rs6897932T allele) and decreased IL-7 availability (hypothesized due to increased IL-7 consumption) were associated with protection against development of autoimmune diseases [10]. Here we demonstrated that also the risk-associated haplotype led to decreased sIL-7Rα serum levels as shown previously [21]. This decrease, however, did not lead to changes in IL-7 serum levels as we showed recently for carriers of the rs1494558-linked rs1494555 SNP [21]. One may speculate about two different explanations for these findings: First, changes in sIL-7Rα expression in risk variant carriers maybe too small to cause increased IL-7 availability. Second additional effects in carriers of protection-associated variants are crucial for increased consumption of IL-7 leading to lower serum levels. In favor of the second thesis, Lundström et al. showed that healthy controls, classified as IL-7Rα protection (or non-protection) haplotype carriers, had no differences in IL-7 serum concentrations, whereas multiple sclerosis patients did [7]. This suggested that crucial differences on the level of IL-7 consuming immune cells exist, which – if IL-7 is more easily accessible – lead to increased IL-7 consumption. In this regard we showed that the protection-associated IL-7Rα variant had marked effects on mIL-7Rα expression in HEK293T cells. Furthermore, comparing both variants concomitantly in HEK293T cells showed dominant mIL-7Rα effects of the Ile244 protective variant. Previous studies did not detect differences of mIL-7Rα expression on T cells but moderately increased mIL-7Rα expression of NK cells in carriers of the protective Ile244 allele was found [11]. One may speculate that regulatory mechanisms of mIL-7Rα internalization (followed by degradation or recycling [22,23]) are involved in counterregulatory mechanisms e.g. to stabilize mIL-7Rα levels. However, this deserves further studies on IL-7Rα *de novo* expression, internalization, as well as recycling and degradation.

5. Conclusions

The results presented here shed a new light on possible mechanisms of how different IL-7Rα variants may contribute to disease susceptibility against autoimmune diseases like T1D.

Declarations of interest

None.

Acknowledgements

We gratefully thank all patients for participating in this study.

Appendix A. Supplementary data

Supplementary data to this article can be found online at https://doi.org/10.1016/j.jaut.2018.10.003.

References

[1] T.J. Fry, C.L. Mackall, The many faces of IL-7: from lymphopoiesis to peripheral T cell maintenance, J. Immunol. 174 (2005) 6571–6576.
[2] H. Dooms, Interleukin-7: fuel for the autoimmune attack, J. Autoimmun. 45 (2013) 40–48.
[3] C.E. Martin, D.S. Spasova, K. Frimpong-Boateng, H.O. Kim, M. Lee, K.S. Kim, et al., Interleukin-7 availability is maintained by a hematopoietic cytokine sink comprising innate lymphoid cells and T cells, Immunity 47 (2017) 171–182 e4.
[4] R. Mazzucchelli, S.K. Durum, Interleukin-7 receptor expression: intelligent design, Nat. Rev. Immunol. 7 (2007) 144–154.
[5] P. Monti, C. Brigatti, M. Krasmann, A.G. Ziegler, E. Bonifacio, Concentration and activity of the soluble form of the interleukin-7 receptor alpha in type 1 diabetes identifies an interplay between hyperglycemia and immune function, Diabetes 62 (2013) 2500–2508.
[6] C.A. Arbelaez, S. Glatigny, R. Duhen, G. Eberl, M. Oukka, E. Bettelli, IL-7/IL-7 receptor signaling differentially affects effector CD4+ T cell subsets involved in experimental autoimmune encephalomyelitis, J. Immunol. 195 (2015) 1974–1983.
[7] W. Lundstrom, S. Highfill, S.T. Walsh, S. Beq, E. Morse, I. Kockum, et al., Soluble IL7Ralpha potentiates IL-7 bioactivity and promotes autoimmunity, Proc. Natl. Acad. Sci. U.S.A. 110 (2013) E1761–E1770.
[8] K.L. Kreft, E. Verbraak, A.F. Wierenga-Wolf, M. van Meurs, B.A. Oostra, J.D. Laman, et al., The IL-7Ralpha pathway is quantitatively and functionally altered in CD8 T cells in multiple sclerosis, J. Immunol. 188 (2012) 1874–1883.
[9] S.G. Gregory, S. Schmidt, P. Seth, J.R. Oksenberg, J. Hart, A. Prokop, et al., Interleukin 7 receptor alpha chain (IL7R) shows allelic and functional association with multiple sclerosis, Nat. Genet. 39 (2007) 1083–1091.
[10] J.A. Todd, N.M. Walker, J.D. Cooper, D.J. Smyth, K. Downes, V. Plagnol, et al., Robust associations of four new chromosome regions from genome-wide analyses of type 1 diabetes, Nat. Genet. 39 (2007) 857–864.
[11] J. Jager, C. Schulze, S. Rosner, R. Martin, IL7RA haplotype-associated alterations in cellular immune function and gene expression patterns in multiple sclerosis, Gene Immun. 14 (2013) 453–461.
[12] E. Hoe, F. McKay, S. Schibeci, R. Heard, G. Stewart, D. Booth, Interleukin 7 receptor alpha chain haplotypes vary in their influence on multiple sclerosis susceptibility

and response to interferon Beta, J. Interferon Cytokine Res. 30 (2010) 291–298.
[13] J. Seyfarth, C. Lundtoft, K. Fortsch, H. Ahlert, J. Rosenbauer, C. Baechle, et al., IL7RA haplotypes differentially affect soluble IL-7 receptor and IL-7 serum concentrations in children with type 1 diabetes, Pediatr. Diabetes 19 (2018) 955–962.
[14] J. Seyfarth, C. Lundtoft, K. Förtsch, H. Ahlert, J. Rosenbauer, C. Baechle, et al., Interleukin-7 Receptor A-chain Haplotypes Differentially Affect Soluble IL-7 Receptor and IL-7 Serum Concentrations in Children with Type 1 Diabetes Pediatric Diabetes, (2018), pp. 1–8.
[15] K. Weber, U. Bartsch, C. Stocking, B. Fehse, A multicolor panel of novel lentiviral "gene ontology" (LeGO) vectors for functional gene analysis, Mol. Ther. 16 (2008) 698–706.
[16] J.R. González, L. Armengol, X. Solé, E. Guinó, J.M. Mercader, X. Estivill, et al., SNPassoc: an R package to perform whole genome association studies, Bioinformatics 23 (2007) 654–655.
[17] C.A. McElroy, J.A. Dohm, S.T.R. Walsh, Structural and biophysical studies of the human IL-7/IL-7rα complex, Structure 17 (2009) 54–65.
[18] S.H. Shakin-Eshleman, S.L. Spitalnik, L. Kasturi, The amino acid at the X position of an Asn-X-ser sequon is an important determinant of N-linked core-glycosylation efficiency, J. Biol. Chem. 271 (1996) 6363–6366.
[19] P. Siupka, O.T. Hamming, L. Kang, H.H. Gad, R. Hartmann, A conserved sugar bridge connected to the WSXWS motif has an important role for transport of IL-21R to the plasma membrane, Gene Immun. 16 (2015) 405–413.
[20] O.J. Hamming, L. Kang, A. Svensson, J.L. Karlsen, H. Rahbek-Nielsen, S.R. Paludan, et al., Crystal structure of interleukin-21 receptor (IL-21R) bound to IL-21 reveals that sugar chain interacting with WSXWS motif is integral part of IL-21R, J. Biol. Chem. 287 (2012) 9454–9460.
[21] J. Seyfarth, C. Lundtoft, K. Fortsch, H. Ahlert, J. Rosenbauer, C. Baechle, et al., Interleukin-7 receptor alpha-chain haplotypes differentially affect soluble IL-7 receptor and IL-7 serum concentrations in children with type 1 diabetes, Pediatr. Diabetes 19 (2018) 955–962.
[22] C.M. Henriques, J. Rino, R.J. Nibbs, G.J. Graham, J.T. Barata, IL-7 induces rapid clathrin-mediated internalization and JAK3-dependent degradation of IL-7Ralpha in T cells, Blood 115 (2010) 3269–3277.
[23] E.M. Faller, S.M. Sugden, M.J. McVey, J.A. Kakal, P.A. MacPherson, Soluble HIV Tat protein removes the IL-7 receptor alpha-chain from the surface of resting CD8 T cells and targets it for degradation, J. Immunol. 185 (2010) 2854–2866.